A DNA nanomachine that maps spatial and temporal pH changes inside living cells

Souvik Modi, Swetha M. G., Debanjan Goswami, Gagan D. Gupta, Satyajit Mayor and Yamuna Krishnan*

DNA nanomachines are synthetic assemblies that switch between defined molecular conformations upon stimulation by external triggers. Previously, the performance of DNA devices has been limited to *in vitro* applications. Here we report the construction of a DNA nanomachine called the I-switch, which is triggered by protons and functions as a pH sensor based on fluorescence resonance energy transfer (FRET) inside living cells. It is an efficient reporter of pH from pH 5.5 to 6.8, with a high dynamic range between pH 5.8 and 7. To demonstrate its ability to function inside living cells we use the I-switch to map spatial and temporal pH changes associated with endosome maturation. The performance of our DNA nanodevices inside living systems illustrates the potential of DNA scaffolds responsive to more complex triggers in sensing, diagnostics and targeted therapies in living systems.

DNA provides remarkable specificity and versatility in the field of molecular recognition and therefore comprises an excellent nanoscale building-block for the creation of precisely self-assembled nanostructures[1]. DNA nanomachines are artificially designed assemblies that change their states in response to inputs such as chemical stimuli generated by environmental cues[1–3]. They can be used as sensors, motors or for logical analysis of gene expression *in vitro*[4–6]. Artificial DNA-based nanoswitches have made use of mechanisms such as differential hybridization, aptamer binding and transition metal ions *in vitro* to effect a diverse set of conformational changes[7–9]. The naturally occurring nanomachines that make up cellular machinery work in tandem with one another to facilitate cellular processes. Importantly, in this molecularly crowded environment, the nanoscale independent function of each machine is converted to an output on the micrometre scale[10]. Of the several bio-inspired nanodevices so far[11,12], DNA nanomachines have proved most attractive for investigation due to their programmability and biocompatibility. However, the successful application of such artificially designed nanomachines inside living cells has not yet been demonstrated, suggesting that the coupling of the nanoscale function of such designed devices to a specific cellular cue is non-trivial. We present the first example of an autonomous DNA nanomachine responsive to a specific molecular trigger, generated within a living cell, and performing its designated task within the molecularly crowded and dynamically changing cellular environment with the same efficacy as it does *in vitro*.

This DNA nanodevice has cytosine-rich regions that function as sensors for chemical input in the form of protons. Cytosine-rich oligonucleotides associate under acidic conditions to form an i-tetraplex[13] consisting of two parallel-stranded C·H·C$^+$ base-paired duplexes that are intercalated in an antiparallel orientation. The present DNA assembly is a robust pH-triggered nanoswitch with fast response times, sustained efficiency over several cycles, and a working cycle that does not generate toxic byproducts. This switch functions as a pH sensor for the range pH 5.5–6.8, which is ideal for monitoring changes in intracellular pH. During endocytosis, acidification has a major role in facilitating cargo dissociation from receptors or in mediating cellular entry of toxins

and viruses[14,15]. The I-switch recapitulates with high fidelity its *in vitro* pH response inside cells, illustrated by the capture of spatiotemporal pH changes associated with endosomal maturation in living cells.

Design and working principle of the I-switch

The I-switch consists of three oligonucleotides O1, O2 and O3, where O1 and O2 are hybridized onto sites adjacent to O3, leaving a one-base gap as shown in Fig. 1a. O1 and O2 have single-stranded cytosine-rich overhangs (see Supplementary Fig. S1) designed such that each overhang forms one-half of a bimolecular i-motif. At acidic pH, these overhangs are protonated and the assembly can fold to form an intramolecular i-motif (Fig. 1a).

In vitro characterization of the I-switch

Circular dichroism (CD) spectroscopy on the I-switch shows that this assembly adopts an extended conformation at pH 7.3, whereas at pH 5 the single-stranded overhangs form an i-motif, yielding a 'closed state' (see Supplementary Fig. S2). The I-switch, fluorescently labelled at its 3′ and 5′ termini with Alexa-488 and Alexa-647 on O1 and O2 respectively, shows fluorescence resonance energy transfer (FRET)[16] at pH 5, with a transfer efficiency of 54–60% consistent with an interfluorophore distance of 4.6 ± 0.5 nm. This is in agreement with the theoretical estimate of 4 nm for the end-to-end distance in such an i-motif. No significant FRET was observed in the open state at pH 7.3 (see Supplementary Fig. S3). FRET was further confirmed through time-resolved fluorescence measurements (Fig. 1d, inset) of the donor in the closed and open states. At pH 7.3, donor lifetimes of the Alexa-488-labelled I-switch showed only a marginal difference between the donor-only-labelled I-switch (~3.77 ns) and the doubly-labelled (Alexa-488/Alexa-647) complex (~3.50 ns). However, at pH 5, the donor lifetime showed a significant change to 2.1 ns for the doubly-labelled I-switch, with the donor-only I-switch showing only a slight decrease (~3.02 ns) (see Supplementary Fig. S4). To see if the I-switch could switch reversibly between the 'closed' and 'open' states upon variation of pH, 5 nM of doubly-labelled I-switch (Alexa-546/647 FRET pair) in 100 mM KCl was subjected to pH cycling between pH 5 and 8 by adding acid or base to the
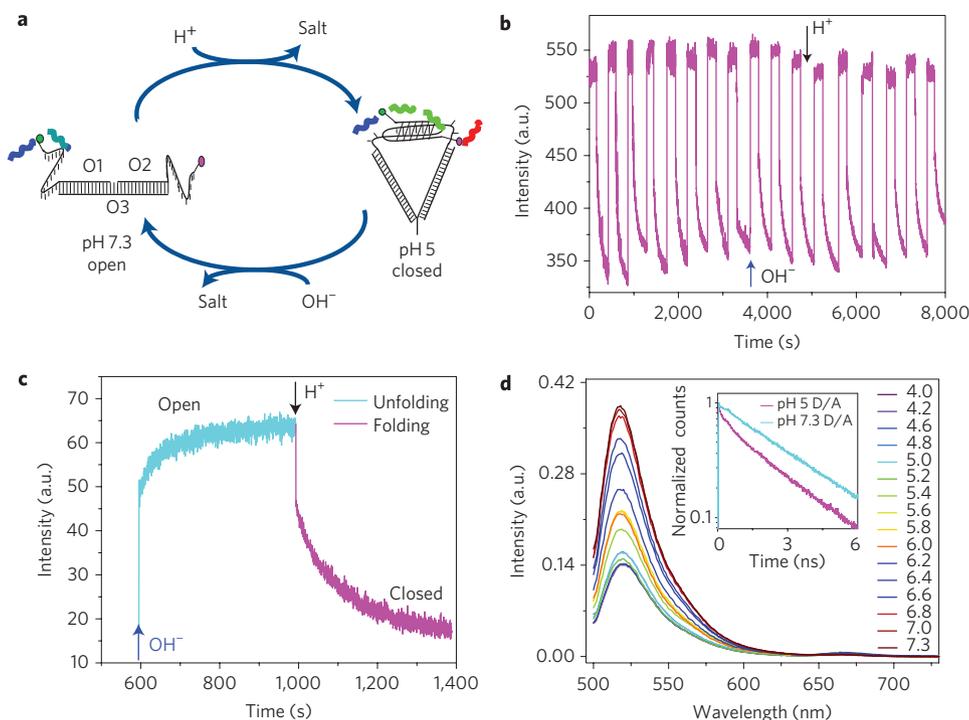

National Centre for Biological Sciences, Tata Institute of Fundamental Research, GKVK, Bellary Road, Bangalore, 560065, India. *e-mail: yamuna@ncbs.res.in

Figure 1 | *In vitro* characterization of the I-switch. a, Schematic of the working principle of the I-switch in the 'open' state (low FRET) at high pH and in the 'closed' state (high FRET) at low pH. **b**, pH cycling of the I-switch in 100 mM KCl, showing donor fluorescence intensity upon alternate addition of acid (black arrow) and base (blue arrow) corrected for dilution. **c**, Representative traces of response time for the formation of the open (cyan) and closed (magenta) states of the switch in response to pH change. The sequential addition of base and acid is shown by blue and black arrows, respectively. **d**, Fluorescence profile of the Alexa-488/647 labelled I-switch (80 nM) in buffer at pH 4–7.3 *in vitro*. Inset, Time-resolved fluorescence spectra of the Alexa-488/647 labelled I-switch at pH 5 and 7.3.

solution (Fig. 1b). Donor fluorescence at 570 nm was followed over time. At high pH, donor fluorescence of the open state was high. At pH 5, this decreased as a result of FRET due to closed state formation, as expected. Switching was highly reversible over at least 20 cycles, with negligible change in efficiency. The response times of the I-switch are moderately fast ($T_{1/2closing} \approx 75$ s, $T_{1/2opening} \approx <3$ s, Fig. 1c).

The pH calibration curve of the I-switch

The fluorescence properties of the I-switch were investigated as a function of pH to determine its range of pH sensitivity (Fig. 1d). Variation in pH on the doubly (Alexa-488/Alexa-647) labelled I-switch changed the ratio between its closed and open states. This resulted in different ratios of the donor and acceptor intensities (D/A) due to FRET in the closed state because of i-motif formation. A plot of D/A as a function of pH (Fig. 2a) shows a standard *in vitro* pH calibration curve for the I-switch that indicates a sigmoid increase between pH 5.0 and 6.8. This was further confirmed by using another FRET pair, Bodipy TMR/Alexa-647, which demonstrated identical ranges of pH sensitivity (see Supplementary Fig. S5). This reaffirmed that the pH sensitivity is not due to the fluorophores, but to the pH response of the underlying DNA scaffold, which is also consistent with other unimolecular i-motif switches[17,18]. The Alexa-488/647-labelled I-switch showed a ~5.5-fold increase *in vitro*, revealing an unprecedented dynamic range between pH 6 and 7. This leaves it well positioned to track fine pH changes associated with endosomal maturation[19].

I-switch and endocytosis

Cellular processes such as endocytosis show characteristic acidification profiles that are integral to endosome maturation, vesicle and cargo functions such as sorting of secretory molecules, growth

factors, nutrients and toxins (see Supplementary Fig. S6 for a schematic)[15]. As early endosomes mature to late endosomes and finally to lysosomes, they undergo a characteristic change of pH ranging from 6 to 6.2 in early endosomes, to pH 5.5 in late endosomes and pH 5 in lysosomes[20]. We therefore investigated the capacity of the I-switch to function inside living cells by investigating endosome maturation in *Drosophila* haemocytes. *Drosophila* haemocytes were 'pulsed' or incubated with a mixture of I-switch labelled with Bodipy TMR (80 nM) and fluorescein isothiocyanate (FITC)-conjugated dextran (FITC-dextran) (1 mg ml^{-1}), a marker of the endosomal fluid phase[21]. Figure 2c shows an image of *Drosophila* haemocytes pulsed (5 min) and chased for 5 min, fixed and then imaged in a confocal microscope. Importantly, the I-switch was found to be localized in distinct punctate structures ~1 μm in size. When these images were overlaid with co-internalized FITC–dextran images, these puncta were found to co-localize (~90%), indicating that the I-switch indeed entered endosomes (Fig. 2c). To check the integrity of the I-switch in living cells over the time period required for endosomal maturation, we next followed the I-switch inside endosomes for periods of 5 min, 1 h and 2 h. Up to 2 h, the donor and acceptor labels of the I-switch remain co-localized in endosomes, indicating the integrity of the I-switch (see Supplementary Fig. S7a). This observation was further confirmed by fluorescence lifetime experiments inside endosomes, supporting that the fluorophores on the I-switch are within FRETting distance (see Supplementary Table S2B).

Spatiotemporal pH mapping of the ALBR endocytic pathway

The pH changes along different endocytic pathways have been measured in various ways[22–24], although this has not been done for the anionic ligand binding receptor (ALBR) pathway. It is
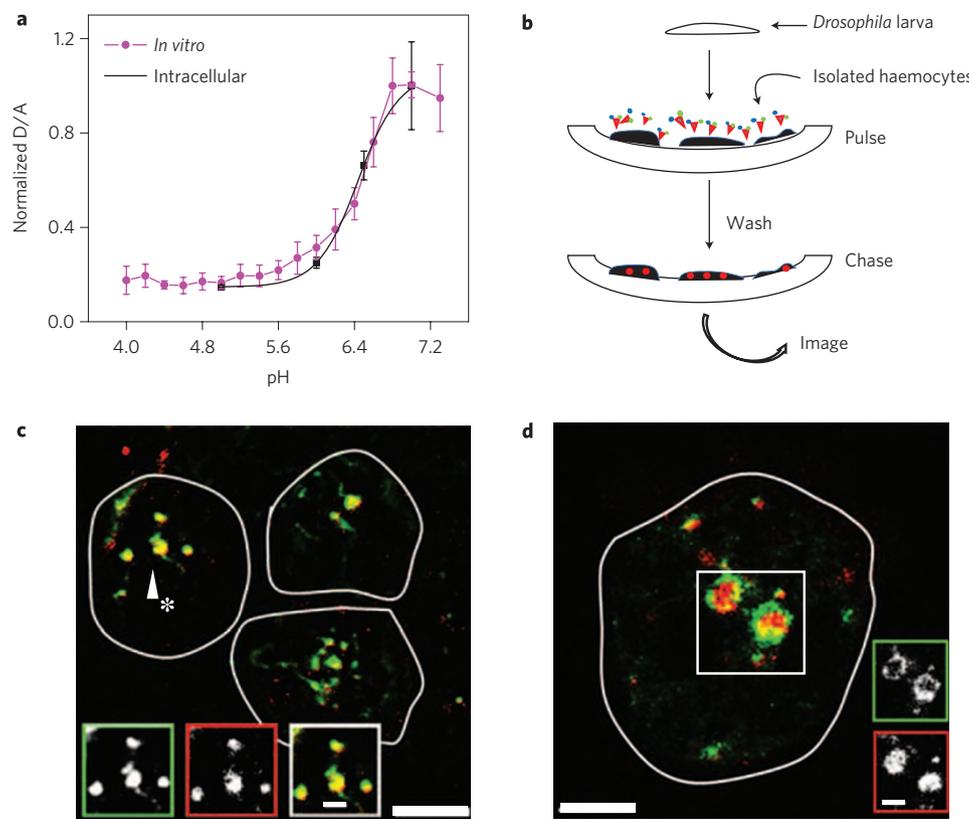
Figure 2 | I-switch internalization and function within endosomes of *Drosophila* haemocytes. a, Haemocytes were pulsed for 5 min, clamped at various pH values between pH 5 and 7 through the external addition of 10 μM Nigericin, fixed and then imaged on a wide-field microscope. The normalized donor/acceptor (D/A) intensity (Alexa-488/Alexa-647) ratios inside the endosomes, plotted as a function of pH, yield the intracellular calibration curve (black), which is overlayed on the *in vitro* pH profile (red). Error bars indicate the mean of two independent experiments ± s.e.m. **b**, Schematic of the labelling assay. *Drosophila* haemocytes were incubated for 5 min with the I-switch (80 nM, 100 μl), which was then removed by washing and imaging at specified times. **c**, Co-localization of the I-switch (red) with endocytic vesicle marker FITC–dextran (green). Cells were pulsed with a solution of FITC–dextran and Bodipy-TMR labelled I-switch, chased and then imaged under a confocal microscope. **d**, Co-localization of endocytosed I-switch (red) with Rab-5-GFP (green) positive endosomes. Confocal image of fixed Rab-5-GFP *Drosophila* haemocytes pulsed with I-switch after a 5 min chase. Scale bar, 5 μm. The insets to **c** and **d** show grey scale, red and green channel images of areas indicated by the asterisk and box respectively. Scale bars, 1 μm.

known that cargo entering cells by means of endocytic pathways such as the ALBR pathway fuse with FITC–dextran-labelled endosomes at the indicated chase times[21]. Competition experiments with maleylated BSA (mBSA) have indicated that the I-switch is internalized through the ALBR-mediated pathway (see Supplementary Fig. S7b). This was re-affirmed by co-localization of the I-switch (Bodipy-TMR/Alexa-647) with the Rab-5-GFP fusion protein (Fig. 2d), which marks early endosomes. We made use of the ratiometric fluorescence property of the I-switch to determine the pH of these endosomes. First, an intracellular standard curve was generated by clamping the pH of endosomes marked with Alexa-488/Alexa-647-labelled I-switch to that of an externally added buffer containing nigericin at high K^+ ion concentration[25]. Endosomal D/A ratios as a function of pH presented a sigmoid profile with a fivefold increase from pH 5 to 7 (Fig. 2a). The intracellular standard D/A curve showed excellent correspondence with the *in vitro* curve, indicating that the I-switch recapitulates its closing and opening characteristics inside cells both qualitatively and quantitatively. To map spatiotemporal changes in endosomal pH, D/A ratios of endosomes were measured at the various chase times of 5 min, 1 h and 2 h after pulsing with the I-switch (Fig. 3a). The D/A ratios calculated at each pixel were colour-coded using Matlab, with blue (D/A = 1) to red (D/A = 0.1) representing the progressive transition from physiological pH to more acidic values. D/A values at each endosome were collected and a spread of the D/A values at each time point shown in a histogram

(Fig. 3b). This indicates a pH of ~6 for the early endosome, pH 5.5 for the late endosome and pH 5 upon fusion with the lysosome (see Supplementary Fig. S8). As expected, endosomes at $t = 5$ min are mildly acidic and progressively acidify over time. The I-switch can also be used to visualize pH changes in real time. We could capture a rapid acidification[26] early in the endosomal maturation process from time-dependent pH measurements (Fig. 3d) where a sharp decrease in D/A is observed over a period of 30 min followed by a slower decrease over 2 h, suggesting that early endosomes in this pathway rapidly acidify to form the late endosome, which then slowly matures to the lysosome. Thus the I-switch reports spatiotemporal pH changes efficiently where variation in pH is a well-defined correlate of molecular processes associated with endosome maturation.

Tracking pH changes for a given protein

To make the I-switch valid as a FRET-based sensor of spatiotemporal pH changes in the environment of a protein of interest, we have developed a strategy to tag it to any given biotinylated protein. We have demonstrated proof of concept by marking the receptor-mediated endocytic (RME) pathway of transferrin[24] in *Drosophila* SR+ cells by tagging the I-switch to transferrin (Fig. 4a). Biotinylated I-switch (I_B) was first conjugated to streptavidin (SA), which was subsequently conjugated to biotinylated transferrin (Tf_B) to yield transferrin-modified I-switch ($I_{B-SA}–Tf_B$)
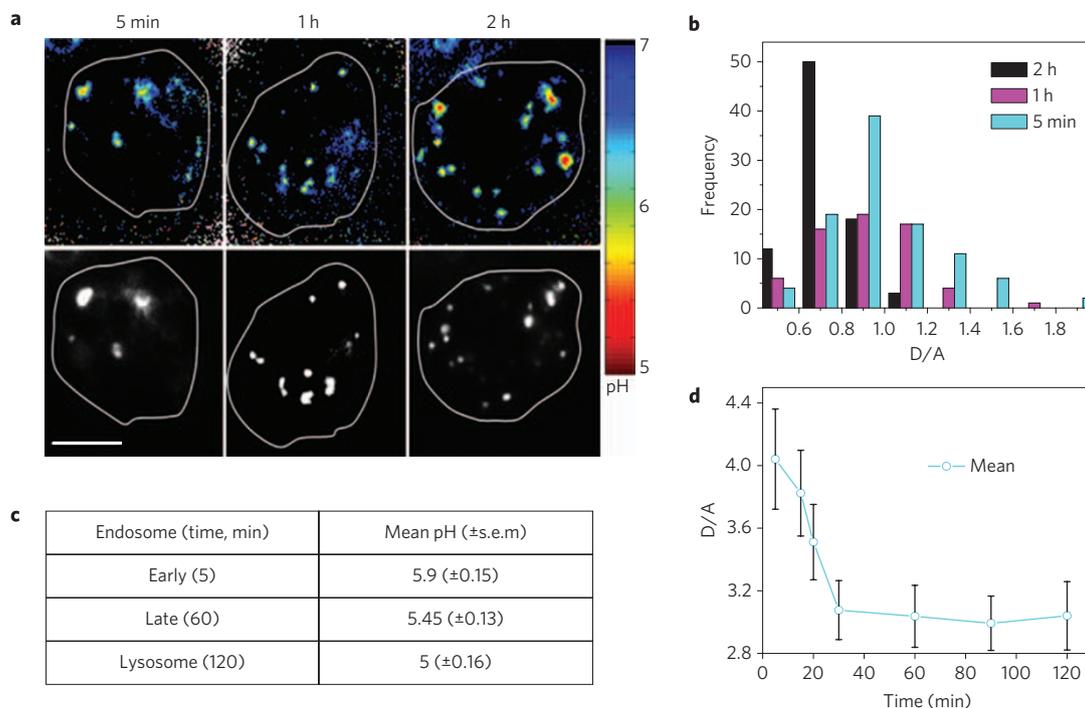
Figure 3 | Spatial and temporal mapping of pH changes during endocytosis using the I-switch in living cells. a, Pseudocolour D/A map of haemocytes pulsed with I-switch (Alexa-488/647) at the indicated chase times. Scale bar, 5 μm. **b,** Histograms showing D/A ratios of ∼80 individual endosomes after chase times of 5 min, 1 h and 2 h. **c,** The table summarizes endosomal pH variation as a function of time. The observed D/A values were converted to their corresponding pH values from the intracellular calibration curve in Fig. 2a. **d,** Real-time monitoring of the rate of acidification during endocytosis. Cells were pulsed with I-switch, washed, then imaged over 2 h. Five distinct cells were imaged for each time point and mean D/A of two experiments was plotted with time. Error bars represent the standard error of the mean. Scale bar, 5 μm.

(Fig. 4a) characterized by gel electrophoresis and size exclusion chromatography (Fig. 4a; see also Supplementary Figs S9 and S10).

Drosophila SR$^+$ cells were incubated with I_{B-SA}–Tf$_B$ (Alexa-488/647-labelled I_B) on ice for 15 min, chased for 10 min, the surface-bound probe was then stripped using a low-pH stripping buffer, fixed and then imaged. Overlaying donor and acceptor images show co-localization in discrete punctate structures (Fig. 4b). These were completely absent in control cells pulsed with the I-switch lacking Tf$_B$. This was further confirmed by competition experiments with unlabelled transferrin (see Supplementary Fig. S11). Transferrin marks recycling endosomes that are comparatively less acidic than the late endosomes and lysosomes. Figure 4c, d shows FRET maps of recycling endosomes marked with I_{B-SA}–Tf$_B$ at $t = 20$ min before (Fig. 4c) and after (Fig. 4d) addition of nigericin. The fold increase of D/A value (blue, pH 5, to red, pH 7) (Fig. 4d) was used to quantify the acidity in these organelles. Before quantification, a pH calibration curve of I_{B-SA}–Tf$_B$ was generated in this cell line as described earlier; this was shown to overlap with the *in vitro* pH curve (Fig. 4 g) indicating that the pH sensing capability of the I-switch is unchanged after conjugation. When the D/A values of each endosome ($n \approx 50$) were quantified and compared with the standard curve, it revealed a mean pH of 6.3 ± 0.1 (Fig. 4 g, black square) which is consistent with the mildly acidic nature of recycling endosomes. This reveals that the I-switch is a high-performance reporter that, through protein conjugation, is able to measure the pH of its environment.

Conclusions

We have demonstrated the successful operation of an artificially designed DNA nanomachine inside living cells, and have shown that these nanomachines work as efficiently inside cells as *in vitro*. Importantly, because the byproducts of a complete cycle for the I-switch are nontoxic, being water and salt, they do not hamper its processivity. The I-switch has a pH sensitivity between pH 5.5 and 6.8 and offers complementary information to that obtained through the use of small-molecule fluorescent pH probes[27,28]. Unlike such pH probes, the I-switch is a FRET-based sensor that is equally bright at both physiological and acidic values of pH. It is also photostable and is a ratiometric probe. Most importantly, with pH probes based on green fluorescent proteins (GFPs)[22] or small molecules one is limited by a fixed wavelength, but the I-switch, which is an artificially designed DNA scaffold, can incorporate any appropriate FRET pair. It can therefore be used to simultaneously follow multiple proteins, with each protein bearing a distinct FRET pair, thus defining it as a powerful probe to study compartment mixing in intracellular sorting or trafficking events. The response of the I-switch is on timescales of 1–2 min, allowing it to be used as a reporter of fine spatial and temporal pH changes associated with biological processes that occur on longer timescales, such as pH variations associated with viral infections[29], phagocytosis[30], chemotaxis[31], apoptosis[32] and defective acidification in tumour cells[33].

This first generation of DNA nanoswitches, although promising, must overcome some limitations before they can be as widely used as current pH sensors. Faster DNA switches that can measure pH changes on shorter timescales, as well as over different ranges of pH sensitivity, need to be engineered. Most importantly, to address compartment mixing issues, methods to specifically target such DNA nanostructures to different cellular organelles would be a crucial development. It is notable that, in analogy to cellular machines, artificially designed DNA nanomachines are responsive to a molecular cue, can be specifically coupled to the cellular environment, and yet function independently within the crowded cellular milieu. Thus, DNA nanomachine function on the nanoscale can be efficiently transduced to cellular length scales. The robustness and level of performance of DNA nanomachines open up a
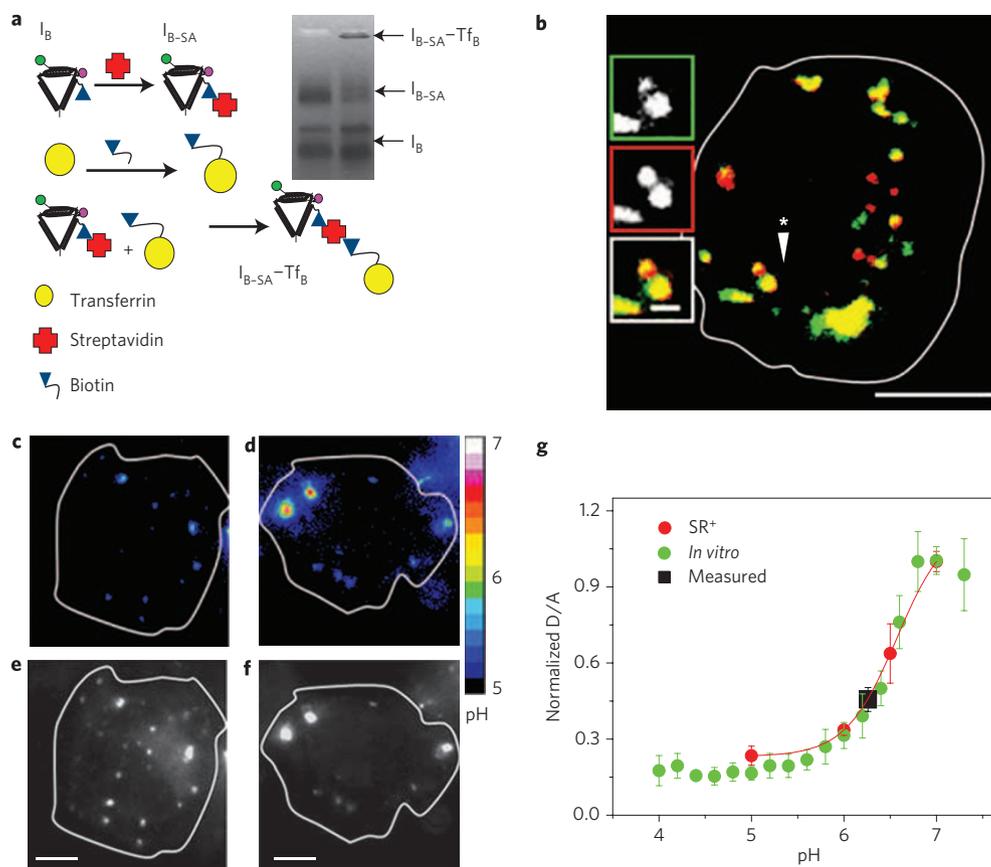
Figure 4 | Protein tagging and pH mapping using the I-switch. a, Tagging strategy to label a specific endocytic pathway with the I-switch (Alexa-488/647). Biotinylated I-switch (I_B) was tagged to biotinylated transferrin (Tf_B) through streptavidin (SA), thus labelling the transferrin with the I-switch. Inset: 3% agarose–TAE gel showing the I-switch–SA conjugate (I_{B-SA}) and the I-switch–SA–transferrin conjugate (I_{B-SA}–Tf_B). **b,** *Drosophila* SR$^+$ cells were pulsed with I-switch–transferrin conjugate (I_{B-SA}–Tf_B, Alexa-488/647-labelled), chased and then imaged under a confocal microscope. **c,** pH maps of I_{B-SA}–Tf_B-labelled endosomes in SR$^+$ cells after a 20-min pulse. **d,** Image of similarly labelled cells after elevation to pH 7 by the addition of 10 μM nigericin. **e,f,** Corresponding intensity images of the cells in **c** and **d**, respectively, in the donor channel. **g,** pH measurements in recycling endosomes. The standard curve in SR$^+$ cells (red) was obtained as previously described, overlayed with the *in vitro* curve (green). Also shown is the experimentally determined pH in recycling endosomes (black square). Values are the mean of two independent experiments ± s.e.m. Scale bars, 5 μm (scale bar in inset, 1 μm).

wide range of possibilities for DNA-based cellular devices for sensing, diagnostics and targeted therapies in living systems.

Methods

Materials. DNA oligonucleotides purified by high-performance liquid chromatography (O1, O2 and O3) were purchased from MWG Biotech. All CD scans were performed on a JASCO J-815 spectrophotometer equipped with a temperature controller at 1 μM strand concentration in the appropriate buffer. Spectra are presented as an average of five successive scans. For fluorescence, samples were excited at 488 nm and emission was collected between 505 nm and 750 nm on a Fluorolog-Spex or a JASCO 815 spectrophotometer. The FRET efficiencies were calculated using the formula $E = 1 - I_{DA}/I_D = 1/[1 + (R/R_o)^6]$. The ratio of intensities at 520–665 nm was plotted against pH for the *in vitro* standard curve. For pH cycling, I-switch solution (5 nM) was switched between pH 5 and 8 by the alternate addition of 3 μl of 0.5 N HCl and 4 μl of 0.5 N KOH.

Cell culture, protein conjugation and imaging. Haemocytes were obtained from wandering third instar *Drosophila* larvae as described previously[21]. For pH measurement experiments, cells were imaged live, after chasing the probes for the stated timepoints. For co-localization of Rab-5 with the I-switch, transgenic flies expressing Rab-5–GFP were crossed to flies expressing Heme–Gal4, and GFP-positive progeny were used for haemocyte cell culture. Stable lines of *Drosophila* SR$^+$ cells expressing the human transferrin receptor (Gupta *et al.*, unpublished) were used for labelling experiments. Wide-field and confocal images were collected using a Nikon inverted microscope and an Olympus Fluoview 1000 confocal microscope respectively. Donor and acceptor images were overlayed and endosomes showing co-localization were further quantified using ImageJ. Five independent measurements were presented as the mean ± standard error (s.e.). I_B comprising O1, O2 and 5′-biotinylated O3 was conjugated to SA in a 1:1 ratio. I_{B-SA} was conjugated to Tf_B similarly in an I_{B-SA}:Tf_B ratio of 1:2. For details see Supplementary Information.

References

1. Bath, J. & Turberfield, A. J. DNA nanomachines. *Nature Nanotech.* **2,** 275–284 (2007).
2. Shih, W. Biomolecular self-assembly: Dynamic DNA. *Nature Mater.* **7,** 98–100 (2008).
3. Yurke, B., Turberfield, A. J., Mills, A. P. Jr, Simmel, F. C. & Neumann, J. L. A DNA-fuelled molecular machine made of DNA. *Nature* **406,** 605–608 (2000).
4. Liu, J. & Lu, Y. A colorimetric lead biosensor using DNA enzyme-directed assembly of gold nanoparticles. *J. Am. Chem. Soc.* **125,** 6642–6643 (2003).
5. Alberti, P. & Mergny, J.-L. DNA duplex–quadruplex exchange as the basis for a nanomolecular machine. *Proc. Natl Acad. Sci. USA.* **100,** 1569–1573 (2003).
6. Benenson, Y., Gil, B., Ben-Dor, U., Adar, R. & Shapiro, E. An autonomous molecular computer for logical control of gene expression. *Nature* **429,** 423–428 (2004).
7. Yin, P., Choi, H. M. T., Calvert, C. R. & Pierce, N. A. Programming biomolecular self-assembly pathways. *Nature* **451,** 318–322 (2008).
8. Beyer, S. & Simmel, F. C. A modular DNA signal translator for the controlled release of a protein by an aptamer. *Nucleic Acids Res.* **34,** 1581–1587 (2006).
9. Mao, C., Sun, W., Shen, Z. & Seeman, N. C. A nanomechanical device based on the B-Z transition of DNA. *Nature* **397,** 144–146 (1999).
10. Allan, V. J. & Schroer, T. A. Membrane motors. *Curr. Opin. Cell Biol.* **11,** 476–482 (1999).
11. Griesbeck, O. Fluorescent proteins as sensors for cellular functions, *Curr. Opin. Neurobiol.* **14,** 636–641 (2004).
12. Ai1, H. W., Hazelwood, K. L., Davidson, M. W. & Campbell, R. E. Fluorescent protein FRET pairs for ratiometric imaging of dual biosensors. *Nature Methods* **5,** 401–403 (2008).

13. Gehring, K., Leroy, J.-L. & Guéron, M. A tetrameric DNA structure with protonated cytidine–cytidine base pairs. *Nature* **363,** 561–565 (1993).
14. Mukherjee, S. Ghosh, R. N. & Maxfield, F. R. Endocytosis. *Physiol. Rev.* **77,** 759–803 (1997).
15. Montesano, R., Roth, J., Robert, A. & Orci, L. Non-coated membrane invaginations are involved in binding and internalization of cholera and tetanus toxins. *Nature* **296,** 651–653 (1982).
16. Stryer, L. & Haugland, R. P. Energy transfer: a spectroscopic ruler. *Proc. Natl Acad. Sci. USA* **58,** 719–726 (1967).
17. Liu, D. & Balasubramanian, S. A proton-fuelled DNA nanomachine. *Angew Chem. Int. Ed.* **42,** 5734–5736 (2003).
18. Liedl, T. & Simmel, F. C. Switching the conformation of a DNA molecule with a chemical oscillator. *Nano Lett.* **5,** 1894–1898 (2005).
19. Ohkuma, S. & Poole, B. Fluorescence probe measurement of the intralysosomal pH in living cells and the perturbation of pH by various agents. *Proc. Natl Acad. Sci. USA* **75,** 3327–3331 (1978).
20. Overly, C. C., Lee, K. D., Berthiaumet, E. & Hollenbeck, P. J. Quantitative measurement of intraorganelle pH in the endosomal–lysosomal pathway in neurons by using ratiometric imaging with pyranine. *Proc. Natl Acad. Sci. USA* **92,** 3156–3160 (1995).
21. Guha, A., Sriram, V., Krishnan, K. S. & Mayor, S. Shibire mutations reveal distinct dynamin-independent and -dependent endocytic pathways in primary cultures of *Drosophila* hemocytes. *J. Cell Sci.* **116,** 3373–3386 (2003).
22. Miesenbock, G., De Angelis, D. A. & Rothman, J. E. Visualizing secretion and synaptic transmission with pH-sensitive green fluorescent proteins *Nature* **394,** 192–195 (1998).
23. Yamashiro, D. J. & Maxfield, F. R. Acidification of morphologically distinct endosomes in mutant and wild-type Chinese hamster ovary cells. *J. Cell Biol.* **105,** 2723–2733 (1987).
24. Sipe, D. M. & Murphy, R. F. High-resolution kinetics of transferrin acidification in BALB/3T3 cells exposed to pH 6 followed by temperature sensitive alkalinization during recycling. *Proc. Natl Acad. Sci. USA* **84,** 7119–7123 (1987).
25. Thomas, J. A., Buschbaum, R. N., Zimniak, A. & Racker, E. Intracellular pH measurements in Ehrlich ascites tumor cells utilizing spectroscopic probes generated *in situ*. *Biochemistry* **18,** 2210–2218 (1979).
26. Murphy, R. F., Powers, S. & Cantor, C. R. Endosome pH measured in single cells by dual fluorescence flow cytometry: rapid acidification of insulin to pH 6. *J. Cell Biol.* **98,** 1757–1762 (1984).
27. Roberta, L. G. & Acosta, D. Ratiometric measurement of intracellular pH of cultured cells with BCECF in a fluorescence multi-well plate reader. *In Vitro Cell. Devel. Biol. Animal* **33,** 256–260 (1997).
28. Koo, M. K., Oh, C. H., Holme, A. L. & Pervaiz, S. Simultaneous analysis of steady-state intracellular pH and cell morphology by automated laser scanning cytometry. *Cytometry A* **71A,** 87–93 (2007).
29. Disbrow, G. L., Hanover, J. A. & Schlegel, R. Endoplasmic reticulum-localized human papillomavirus type 16 E5 protein alters endosomal pH but not *trans*-Golgi pH. *J. Virol.* **79,** 5839–5846 (2005).
30. Downey, G. P. *et al.* Phagosomal maturation, acidification, and inhibition of bacterial growth in nonphagocytic cells transfected with FcγRIIA Receptors *J. Biol. Chem.* **274,** 28436–28444 (1999).
31. Simchowitz, L. & Cragoe, E. J. Jr Regulation of human neutrophil chemotaxis by intracellular pH. *J. Biol. Chem.* **261,** 6492–6500 (1986).
32. Matsuyama, S. & Reed, J. C. Mitochondria-dependent apoptosis and cellular pH regulation. *Cell Death Diff.* **7,** 1155–1165 (2000).
33. Altan, N., Chen, Y., Schindler, M. & Simon, S. M. Defective acidification in human breast tumor cells and implications for chemotherapy. *J. Exp. Med.* **187,** 1583–1598 (1998).

Author contributions

S.M., S.M. and Y.K. conceived, designed and analysed the experiments. S.M. and S.M.G. performed the experiments. S.M. and Y.K. wrote the paper. D.G. performed time-resolved experiments. G.D.G. contributed the SR⁺ cell line.

Additional information

Supplementary information accompanies this paper at www.nature.com/naturenanotechnology. Reprints and permission information is available online at http://npg.nature.com/reprintsandpermissions/. Correspondence and requests for materials should be addressed to Y.K.